



Original article

Design, synthesis and in vitro antitumour activity of new heteroaryl ethylenes

Cosimo G. Fortuna^{a,*}, Vincenza Barresi^a, Carmela Bonaccorso^a, Giuseppe Consiglio^b,
Salvatore Failla^b, Angela Trovato-Salinaro^a, Giuseppe Musumarra^a

^a Dipartimento di Scienze Chimiche, Università degli Studi di Catania, Viale A. Doria 6 95125, Catania, Italy

^b Dipartimento di Ingegneria Industriale e Meccanica, Università degli Studi di Catania, Viale A. Doria 6 95125, Catania, Italy

ARTICLE INFO

Article history:

Received 1 August 2011

Received in revised form

24 October 2011

Accepted 25 October 2011

Available online 11 November 2011

Keywords:

Molecular modelling

Antitumour compounds

Heterocycles

QSAR

ABSTRACT

Almond and VolSurf + modelling procedures allowed the structural design of new di- and mono-heteroaryl-ethylenes. The structural modifications suggested by the molecular modelling were verified by the synthesis of the designed molecules and by the evaluation of their in vitro activities against two lung tumour cell lines, A549 and H226. 2-((E)-2-[5'-(Dibutylamino)-2,2'-bithien-5-yl]vinyl)-1-methylquinolinium iodide exhibited in vitro antiproliferative activity two orders of magnitude higher than that of the most active compound previously synthesized in our laboratory.

© 2011 Elsevier Masson SAS. All rights reserved.

1. Introduction

Previous work on the design, the synthesis and the antitumour activity of new trans 1-heteroaryl-2-(1,3-dimethylimidazolium-2-yl) ethylenes [1] confirmed the hypothesis, based on a Molecular Interaction Field (MIF) [2,3] approach using Grid Independent Descriptors (GRIND) [4], that the presence of three aromatic moieties and of halogen atoms are the main structural features necessary to obtain satisfactory antiproliferative activities. The synthesis, QSAR modelling using the program Almond, and biological [5–8] assays of vinyl and halo-furan derivatives has been reported and their activities as anticancer drugs evaluated together with their toxicity effects [9–12]. Recent work of our group on the design of new trans 2-(furan-2-yl)vinyl heteroaromatic iodides [13] and new trans 2-(thiophen-2-yl)vinyl heteroaromatic iodides [14] using a new chemoinformatic tool, VolSurf+, including both modelling of ADME (Adsorption, Distribution, Metabolism, Elimination) properties in the design of new structures and the correlation 3D molecular fields with physico-chemical and pharmacokinetic properties, was adopted for predicting their in vitro antitumour activities. In this context we here report the design, the synthesis and the biological evaluation of new di- and mono-heteroaryl-ethylenes designed using both Almond and

VolSurf approaches. In this work, we designed some structures with quinolinium, pyridinium and imidazolium salts linked by one or two ethylenic bonds to different substituted aromatic and heteroaromatic moieties. The structural modifications suggested by the molecular modelling approach have been verified by the synthesis of the designed molecules and by the evaluation of their in vitro activities tests against two lung tumour cell lines, A549 and H226.

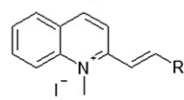
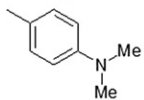
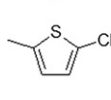
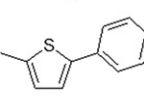
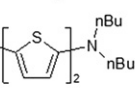
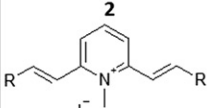
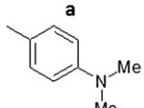
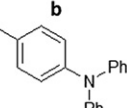
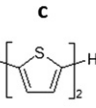
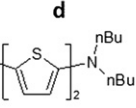
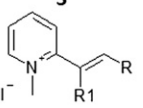
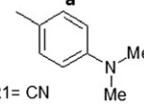
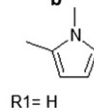
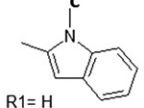
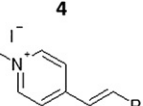
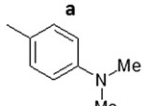
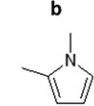
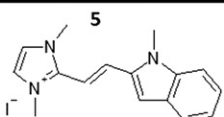
2. Results and discussion

The structures of the compounds reported in Scheme 1 were first modelled selecting a MIF approach, adopting Grid Independent Descriptors calculated using the program Almond, based on the 3D structures following the procedure described in the Computational Methods section. The cyano derivative **3a** was inserted in Scheme 1 as phenylacrylonitriles have recently been reported to display high levels of growth inhibition against several human cancer cell lines [15]. Compound **1c**, the most active previously synthesized in our laboratory, was also imported for comparison.

PCA of ALMOND descriptors relative to compounds in Scheme 1 afforded a 5 PC model explaining 80.3% of variance. In Fig. 1, the scores plot depicting the data structure elucidated by 3 PC (explaining approximately 70% of variance), the most active compound (**1c**), exhibits a positive value in y axis, which can reasonably be assumed as a direction representative of antitumour activities. We can notice that compounds **1d**, **2a**, **2b** and **2c** exhibit higher Y values, while **1a** is comparable with **1c**.

* Corresponding author. Fax: +39095580138.

E-mail address: cg.fortuna@unict.it (C.G. Fortuna).

COMPOUNDS	DESIGNATION				
	R=				
	R=				
	R=	 R1= CN	 R1= H	 R1= H	
	R=				
					

Scheme 1. Structures of the synthesized compounds.

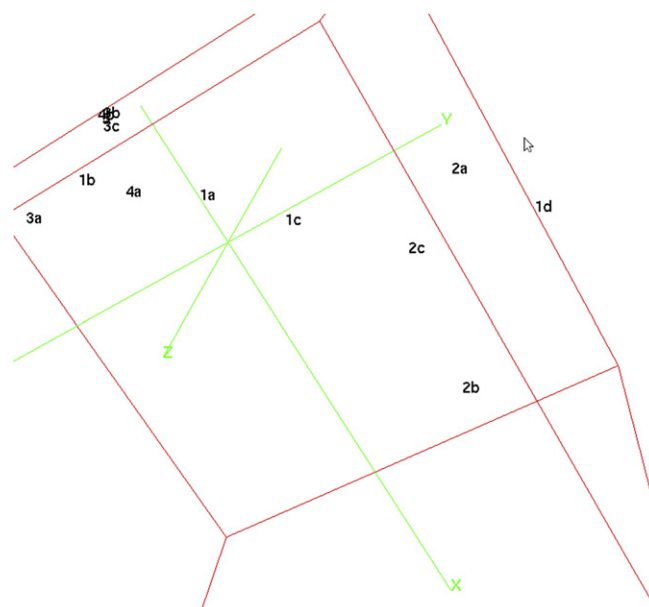
Almond is based on the assumption that the process of ligand–receptor interaction can be represented with the help of MIF. However, an increased drug–receptor interaction does not necessarily imply an increase in biological activity. It is also very important to design new structures which exhibit ADME properties warranting an acceptable bioavailability. A high-throughput chemoinformatic approach should therefore include modelling of ADME properties in the design of new structures. For this purpose, the Volsurf approach, able to correlate 3D molecular structures with physico-chemical properties, appears to be appropriate. Therefore the same frameworks were analysed by a recent development of this methodology called VolSurf+. PCA for the same compounds afforded a 5 PC model explaining 90.3% of variance. In Fig. 2 we report 3D Volsurf PCA scores plot where it is possible to notice a trend similar to Almond, with the same compounds exhibiting positive values along the 1st component.

This finding implies that the designed compounds are expected to exhibit both satisfactory activities and bio-availabilities. In this context we decided to experimentally verify the model indications by synthesizing and testing in vitro the designed compounds spanning a wide range of expected activities. The synthesis of iodides **1–5** is straightforward and can be easily achieved by condensation of pyridinium, quinolinium or imidazolium iodides with heteroaromatic aldehydes (Scheme 2). As expected, the α methyls are quite reactive due to the strong electron withdrawing effect of the adjacent positively charged nitrogen atom.

5'-(Dibutylamino)-2,2'-bithiophene-5-carbaldehyde [16] was synthesized adopting a synthetic procedure involving the direct amidation of the 4-Oxo-4-thiophen-2-yl-butyric acid with N,N-dibutylamine through a DCC-BtOH catalysed reaction followed by treatment of the resulting amide with Lawesson's reagent to give the corresponding N,N-dibutylaminobithiophene. The aldehyde was obtained by metallation, using n-BuLi, followed by quenching with DMF (see Supporting Information). Under appropriate

conditions, outlined in the experimental section, pure trans isomers **1–5** were obtained, as evidenced by the ethylenic protons J coupling constants in the NMR spectra.

The antiproliferative activities of the newly synthesized compounds were then tested against two tumour cell lines of human lung carcinoma, A549 and H226. The in vitro activities, expressed as Log GI₅₀ values (see Experimental Section), are recorded in Table 1, together with that of **1c**, the most active compound in previous in vitro tests. Some designed and

Fig. 1. Three components Almond scores plot for compounds **1–5**.

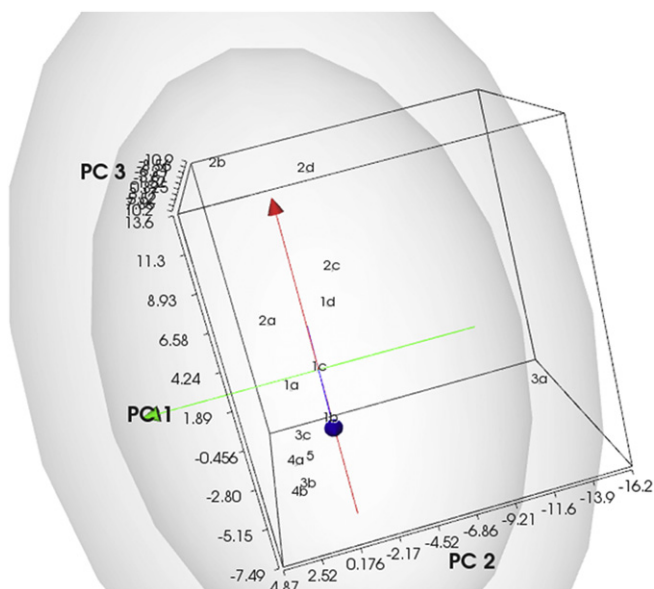
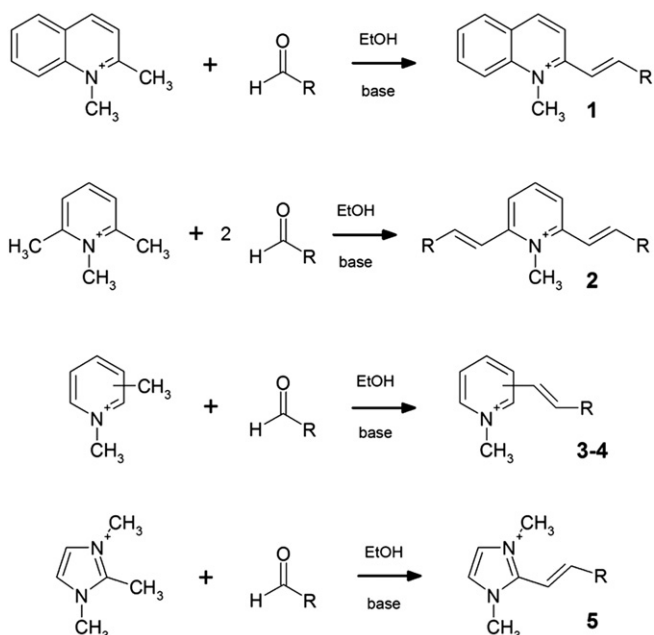


Fig. 2. Three components VolSurf + scores plot for compounds 1–5.

synthesized compounds in Scheme 1 are not reported in Table 1 due to their poor solubility in aqueous solution which prevented a reliable evaluation of their in vitro activities. It is also worth mentioning that, in order to obtain comparable biological tests, Log GI₅₀ were all measured in the same experiment. The percent of growth and the inhibition exerted by different doses (0.01–100 μM) are recorded in Figs. 3 and 4. In addition to antiproliferative effects (Log GI₅₀), in Table 2 cytotoxic activities, expressed as Log LC₅₀ values, are also reported.

Experimental in vitro values in Tables 1 and 2 support the overall picture provided by the Almond and VolSurf + models. In fact compounds 1d and 2a, indicated by the modelling procedures to have a very good activity and bioavailability, are actually the most active ones, exhibiting unprecedented Log GI₅₀ (up to –8 vs A549) values and good cytotoxicities. The validity of the models is



Scheme 2. General procedures for synthesis of compounds 1–5 (see Scheme 1 for R).

Table 1

In vitro antitumour activities for A549 and H226 cell lines.

Compounds/cell lines	A549 ^a	H226 ^a
1a	–5.81	–6.20
1c	–5.70	–5.84
1d	–8.00	–7.34
2a	–6.43	–7.35
2b	–5.50	–5.70
2d	–5.32	–6.00
3a	–5.42	–4.71
3b	–4.64	–4.00
4a	–5.80	–5.00
4b	–5.78	–4.00

^a Expressed as Log GI₅₀.

confirmed by the poor activity of compounds with lower Y values in Figs. 1 and 2. These results confirm that the presence of at least three aromatic/heteroaromatic moieties is needed to obtain good antiproliferative activities, which can be further potentiated by dialkylamino substituents linked to an aromatic ring.

3. Conclusion

This work confirms the potentialities of Almond and VolSurf + modelling procedures, which allowed the structural design of 1d and 2a exhibiting in vitro antitumour activities two orders of magnitude higher than that of 1c, the most active compound previously synthesized in our laboratory. Further structural modifications of 1d, at the present the lead compound for future studies, might produce even better in vitro antitumour activities vs A549.

4. Experimental section

4.1. Computational Methods

4.1.1. VolSurf + descriptors

The interaction of molecules with biological membranes is mediated by surface properties such as shape, electrostatic forces, H-bonds and hydrophobicity. Therefore, the GRID force field was chosen to characterize potential polar and hydrophobic interaction sites around target molecules by the water (OH2), the hydrophobic (DRY), and the carbonyl oxygen (O) and amide nitrogen (N1) probe. The information contained in the MIF is transformed into a quantitative scale by calculating the volume or the surface of the interaction contours. The VolSurf + procedure is as follows: i) in the first step, the 3D molecular field is generated from the interactions of the OH2, the DRY, O and N1 probe around a target molecule; ii) the second step consists in the calculation of descriptors from the 3D

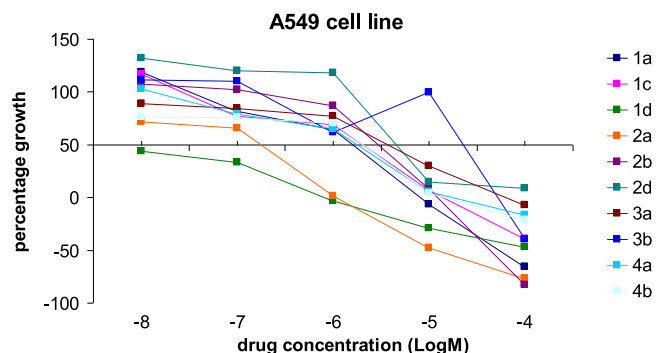


Fig. 3. Dose – response curves of antiproliferative activities vs A549.

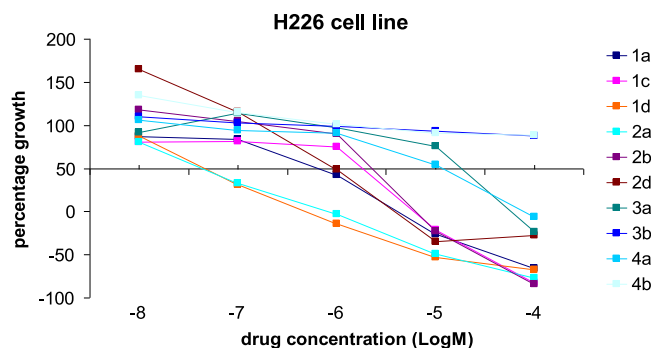


Fig. 4. Dose – response curves of antiproliferative activities vs H226.

maps obtained in the first step. The molecular descriptors obtained, called VolSurf + descriptors, refer to molecular size and shape, to hydrophilic and hydrophobic regions and to the balance between them, to molecular diffusion, LogP, LogD, to the “charge state” descriptors, to the new 3D pharmacophoric descriptors and to some descriptors on some relevant ADME properties [17–20]. Finally, chemometric tools (PCA [21], PLS [22]) are used to create relationships of the VolSurf + descriptor matrix with ADME properties. The scheme of the VolSurf + programme steps and a detailed definition of Volsurf + descriptors have recently been reported [14].

4.1.2. Almond

MIF were obtained using the program GRID version 2.0 [23]. GRIND were generated, analysed, and interpreted using the program Almond version 3.0.0 [24], a software package developed in our group. Computations and graphical display were performed on SGI O2 workstations (MIPS R12000 processor). The process of ligand–receptor interaction has often been represented with the help of the MIF. If a compound is known to bind a certain receptor, some of the regions defined in its Virtual Receptor Site (VRS) [4] should actually overlap groups of the real receptor site and, therefore, at least a subset of the VRS regions would be relevant for representing the binding properties of the ligand. For the latter statement to be true the VRS must have been obtained from the bioactive conformation of the ligand and the probes used to compute it should represent chemical groups present in the binding site. The molecular descriptors presented in this work are based on the concept of VRS. Basically, GRIND are a small set of variables representing the geometrical relationships between relevant regions of the VRS and as such are independent of the coordinate frame of the space where the MIF is computed. The procedure for obtaining GRIND involves three steps: (i) computing a set of MIF, (ii) filtering the MIF to extract the most relevant regions that define the VRS, and (iii) encoding the VRS into the GRIND variables.

4.1.3. Molecular description: GRID Force Field

The GRID program [2,25,26] was used to describe the molecular structures. GRID is a computational procedure for detecting energetically favourable binding sites on molecules. The program calculates the interactions between the molecule and a probe group

which is moved through a regular grid of points in a region of interest around the target molecule and, at each point, the interaction energy between the probe and the target molecule is calculated as the sum of Lennard-Jones (ELJ), hydrogen bond (EHB) electrostatic interactions (EEL) and, for specific probes, entropic contribution (EENT):

$$Ex_{x,y,z} = \sum_{i=1}^N E_{LJ} + \sum_{i=1}^N E_{HB} + \sum_{i=1}^N E_{ENT}$$

GRID contains a table of parameters to describe each type of atom occurring in each of the ligand molecules. These parameters define the strength of the Lennard-Jones, hydrogen bond and electrostatic interactions made by an atom and are used in order to evaluate the energy functions. GRID probes are very specific. They give precise spatial information, and this specificity and sensitivity are an advantage since the probes may then be representative of the important chemical groups present in the active site provided that the statistical method used for the analysis can distinguish between different types of interactions.

4.2. Synthesis

4.2.1. General

All the chemicals were obtained from Sigma Aldrich and used as received. Thin layer chromatography (TLC) was carried out on silica gel plates (Merck 60, F254). All reactions were carried out under nitrogen atmosphere unless otherwise stated. NMR experiments were carried out at 27 °C on a 500 MHz spectrometer (¹H at 499.88 MHz, ¹³C NMR at 125.7 MHz) equipped with a pulse field gradient module (Z axis) and a tunable 5 mm Varian inverse detection probe (ID-PFG); chemical shifts (δ) are expressed in ppm and are referenced to residual undeuterated solvent. NMR data were processed using the MestReC software. Electrospray ionization mass spectra (ESI-MS) were recorded on a Finnigan LCQ Deca XP ion trap (Thermo Fischer Scientific, USA) using an electrospray ionization (ESI) interface. Melting points are uncorrected. 2-(Pyridin-2-yl)acetonitrile, 4-(dimethylamino)benzaldehyde, 5-chlorothiophene-2-carbaldehyde, 2,2'-bithiophene-5-carbaldehyde, 1-methyl-1H-pyrrole-2-carbaldehyde and 1-methyl-1H-indole-2-carbaldehyde were Aldrich commercial products. 5'-(Dibutylamino)-2,2'-bithiophene-5-carbaldehyde [16], 4-(diphenylamino)-benzaldehyde [27], 1,2-dimethylquinolinium iodide [28], 1,2,6-trimethylpyridinium iodide [29], 1,2-dimethyl-picolinium iodide [30], 1,4-dimethyl-picolinium iodide [31] and 1,2,3-trimethylimidazolium iodide [32] were prepared according to the literature.

4.3. General procedure for the synthesis of compounds 1–5

Compounds 1–5, all iodide salts, were obtained by refluxing in ethanol stoichiometric amounts (see Scheme 2) of 1,2-dimethylquinolinium iodide, 1,2,6-trimethylpyridinium iodide, 1,2-dimethyl-picolinium iodide, 1,4-dimethyl-picolinium iodide or 1,2,3-trimethylimidazolium iodide and the appropriate aldehyde in the presence of catalytic amount of piperidine. The resulting precipitates were recrystallized from ethanol. Details on the synthetic conditions and products characterization are reported below.

4.3.1. 2-(Cyanomethyl)-1-methylpyridinium iodide

2-(Pyridin-2-yl)acetonitrile (1.180 g, 10.00 mmol), and iodo-methane (4.26 g, 30.00 mmol) were dissolved in acetonitrile (5 mL), and stirred for 24 h at room temperature. The solid precipitated was collected by filtration and washed with cold acetonitrile to give 2-(cyanomethyl)-1-methylpyridinium iodide as pale-brown needles (1.846 g, 71%); m.p.: 205–207 °C; ¹H NMR (500 MHz [D₆]DMSO):

Table 2
In vitro antitumour activities for A549 and H226 cell lines.

Compounds/cell lines	A549 ^a	H226 ^a
1a	–4.15	–4.20
1c	–	–4.42
1d	–	–5.00
2a	–4.88	–4.86
2b	–4.40	–4.48

^a Expressed as Log LC₅₀.

δ = 4.26 (s, 3H, N⁺CH₃), 4.79 (s, 2H, CH₂CN), 8.11 (t, J = 7.0 Hz, 1H, ArH), 8.17 (d, J = 7.0 Hz, 1H, ArH), 8.63 (t, J = 7.5 Hz, 1H, ArH), 9.07 (d, J = 6.0 Hz, 1H, ArH); ¹³C NMR (126 MHz [D₆]DMSO): δ = 46.96, 106.41, 126.58, 130.35, 134.26, 145.54, 146.82 ppm; MS (positive ESI) m/z (%): 134 (100) [M – I]⁺.

4.3.2. 2-[(E)-2-[4-(Dimethylamino)phenyl]vinyl]-1-methylquinolinium iodide [33], **1a**

The compound was synthesized according to the general procedure using 1,2-dimethylquinolinium iodide (0.570 g, 2 mmol) and 4-(dimethylamino)benzaldehyde (0.298 g, 2.00 mmol) to gave **1a** (0.691 g, 83%).

4.3.3. 2-[(E)-2-(5-Chloro-2-thienyl)vinyl]-1-methylquinolinium iodide, **1b**

The compound was synthesized according to the general procedure using 1,2-dimethylquinolinium iodide (0.150 g, 0.53 mmol) and 5-chlorothiophene-2-carbaldehyde (0.077 g, 0.53 mmol) to gave **1b** as brown needles (0.088 g, 40%); m.p.: 189–191 °C; ¹H NMR (500 MHz [D₆]DMSO): δ = 4.48 (s, 3H, N⁺CH₃), 6.54 (d, J = 3.5 Hz, 1H, ArH), 7.50 (d, J = 16.0 Hz, 1H, CH=CH), 7.14 (d, J = 3.5 Hz, 1H, ArH), 7.93 (t, J = 8.0 Hz, 1H, ArH), 8.17 (t, J = 7.0 Hz, 1H, ArH), 8.30 (d, J = 16.0 Hz, 1H, CH=CH), 8.31 (d, J = 7.0 Hz, 1H, ArH), 8.44 (d, J = 9.0 Hz, 1H, ArH), 8.56 (d, J = 9.0 Hz, 1H, ArH), 9.01 (d, J = 9.0 Hz, 1H, ArH) ppm; ¹³C NMR (126 MHz [D₆]DMSO): δ = 45.15, 119.42, 122.67, 122.91; 122.96; 124.72; 124.79; 126.06; 127.92; 133.21; 135.53; 137.55; 140.58; 140.65; 141.07; 151.57 ppm; MS (positive ESI): m/z (%): 286.2 [M – I]⁺.

4.3.4. 1-methyl-2-[(E)-2-(5-Phenyl-2-thienyl)vinyl]quinolinium iodide [14], **1c**

The compound was synthesized according to the general procedure using 1,2-dimethylquinolinium iodide (0.200 g, 0.70 mmol) and 5-phenylthiophene-2-carbaldehyde to gave **1c** (0.061 g, 30%).

4.3.5. 2-[(E)-2-[5'-(Dibutylamino)-2,2'-bithien-5-yl]vinyl]-1-methylquinolinium iodide [16], **1d**

The compound was synthesized according to the general procedure using 1,2-dimethylquinolinium iodide (0.057 g, 0.2 mmol) and 5'-(dibutylamino)-2,2'-bithiophene-5-carbaldehyde (0.074 g, 0.2 mmol) to gave **1d** (0.054 g, 41%).

4.3.6. 2,6-Bis[(E)-2-[4-(Dimethylamino)phenyl]vinyl]-1-methylpyridinium iodide [34], **2a**

The compound was synthesized according to the general procedure using 1,2,6-trimethylpyridinium iodide (0.248 g, 1.00 mmol) and 4-(dimethylamino)-benzaldehyde (0.298 g, 2.00 mmol) to gave **2a** (0.307 g, 60%).

4.3.7. 2,6-Bis[(E)-2-[4-(diphenylamino)phenyl]vinyl]-1-methylpyridinium iodide, **2b**

The compound was synthesized according to the general procedure using 1,2,6-trimethylpyridinium iodide (0.248 g, 1.00 mmol) and 4-(diphenylamino)benzaldehyde (0.545 g, 2.00 mmol), to gave **2b** as red needles (0.600 g, 79%); m.p.: 230–233 °C; ¹H NMR (500 MHz [D₆]DMSO): δ = 4.23 (s, 3H, N⁺CH₃), 6.96 (d, J = 8.5 Hz, 4H, ArH), 7.11 (d, J = 7.0 Hz, 8H, ArH), 7.16 (t, J = 7.0 Hz, 4H, ArH), 7.38 (t, J = 7.0 Hz, 8H, ArH), 7.46 (d, J = 16.0 Hz, 2H, CH=CH), 7.69 (d, J = 16.0 Hz, 2H, CH=CH), 7.72 (d, J = 8.5 Hz, 4H, ArH), 8.18 (d, J = 8.5 Hz, 2H, ArH), 8.33 (t, J = 8.5 Hz, 1H, ArH) ppm; ¹³C NMR (126 MHz [D₆]DMSO): δ = 153.88, 149.86, 146.75, 142.85, 142.32, 130.43, 130.28, 128.65, 125.66, 124.85, 123.28, 121.40, 116.88, 41.91 ppm; MS (positive ESI): m/z (%): 632.9 [M – I]⁺.

4.3.8. 2,6-Bis[(E)-2-(2,2'-bithien-5-yl)vinyl]-1-methylpyridinium iodide, **2c**

The compound was synthesized according to the general procedure using 1,2,6-trimethylpyridinium iodide (0.100 g, 0.40 mmol) and 2,2'-bithiophene-5-carbaldehyde (0.155 g, 0.80 mmol) to gave **2c** as orange needles (0.053 g, 21%); m.p.: 192–195 °C; ¹H NMR (500 MHz [D₆]DMSO): δ = 4.23 (s, 3H, N⁺CH₃), 7.16 (d, J = 4.0 Hz, 2H, ArH), 7.30 (d, J = 15.5 Hz, 2H, CH=CH), 7.43 (d, J = 3.5 Hz, 2H, ArH), 7.47 (d, J = 3.5 Hz, 2H, ArH), 7.59 (d, J = 4.0 Hz, 2H, ArH), 7.63 (d, J = 5.0 Hz, 2H, ArH), 7.96 (d, J = 15.5 Hz, 2H, CH=CH), 8.20 (d, J = 8.0 Hz, 2H, ArH), 8.37 (t, J = 8.0 Hz, 1H, ArH) ppm; ¹³C NMR (126 MHz, CDCl₃): δ = 44.52, 120.92, 122.48, 122.56, 124.39, 124.94, 128.04, 131.12, 134.70, 137.35, 138.68, 139.71, 142.12, 158.61 ppm; MS (positive ESI): m/z (%): 474.2 [M – I]⁺.

4.3.9. 2,6-Bis-[(E)-2-[5'-(dibutylamino)-2,2'-bithienyl-5-yl]-vinyl]-1-methylpyridinium iodide, **2d**

The compound was synthesized according to the general procedure using 1,2,6-trimethylpyridinium iodide (0.025 g, 0.1 mmol) and 5'-(dibutylamino)-2,2'-bithiophene-5-carbaldehyde (0.074 g, 0.2 mmol) to gave **2d** as dark oil (0.055 g, 65%); ¹H NMR (500 MHz, CDCl₃): δ = 0.97 (t, J = 7.4 Hz, 12H, –CH₃); 1.36 (m, 8H, CH₂); 1.61 (m, 8H, CH₂); 3.21 (t, J = 7.4 Hz, 8H, NCH₂); 4.25 (s, 3H, N⁺CH₃), 5.72 (d, J = 3.3 Hz, 2H, ArH), 6.71 (d, J = 3.3 Hz, 2H, ArH), 6.73 (d, J = 15.5 Hz, 2H, CH=CH), 7.01 (d, J = 4.0 Hz, 2H, ArH), 7.33 (d, J = 4.0 Hz, 2H, ArH), 7.68 (d, J = 15.5 Hz, 2H, CH=CH), 7.90 (d, J = 7.8 Hz, 2H, ArH), 7.98 (t, J = 7.8 Hz, 1H, ArH) ppm; ¹³C NMR (126 MHz [D₆]DMSO): δ = 13.91, 20.24, 29.17, 42.71, 53.36, 101.70, 113.17, 117.99, 120.42, 121.76, 127.02, 134.87, 135.15, 135.42, 141.19, 144.70, 152.62, 159.13 ppm; MS (positive ESI): m/z (%): 729.0 [M – I]⁺.

4.3.10. 2-[(Z)-2-(4-Aminophenyl)-1-cyanovinyl]-1-methylpyridinium iodide, **3a**

The compound was synthesized according to the general procedure using 2-(cyanomethyl)-1-methylpyridinium iodide (0.520 g, 2 mmol) and 4-(dimethylamino)benzaldehyde (0.298 g, 2.00 mmol) to gave **3a** as green-grey needles (0.626 g, 80%); m.p.: 183–185 °C dec.; ¹H NMR (500 MHz [D₆]DMSO): δ = 3.10 (s, 6H, ArNCH₃), 4.36 (s, 3H, N⁺CH₃), 6.89 (d, J = 9.0 Hz, 2H, ArH), 7.80 (s, 1H, CH=C), 7.95 (d, J = 9.0 Hz, 2H, ArH), 8.08 (t, J = 6.5 Hz, 1H, ArH), 8.25 (d, J = 8.0 Hz, 1H, ArH), 8.61 (t, J = 8.0 Hz, 1H, ArH), 9.04 (d, J = 6.5 Hz, 1H, ArH) ppm; ¹³C NMR (126 MHz [D₆]DMSO): δ = 155.47, 153.97, 150.98, 147.81, 146.17, 133.53, 130.31, 127.05, 119.62, 117.56, 112.19, 91.43, 47.39, 40.16 ppm; MS (positive ESI): m/z (%): 265.3 [M – I]⁺.

4.3.11. 1-Methyl-2-[(E)-2-(1-methyl-1H-pyrrol-2-yl)vinyl]pyridinium iodide [35], **3b**

The compound was synthesized according to the general procedure using 1,2-dimethylpyridinium iodide (0.470 g, 2 mmol) and 1-methyl-1H-pyrrole-2-carbaldehyde (0.218 g, 2.00 mmol) to gave **3b** (0.639 g, 98%).

4.3.12. 1-Methyl-2-[(E)-2-(1-methyl-1H-indol-2-yl)vinyl]pyridinium iodide, **3c**

The compound was synthesized according to the general procedure using 1,2-dimethylpyridinium iodide (0.100 g, 0.043 mmol) and 1-methyl-1H-indole-2-carbaldehyde (0.065 g, 0.043 mmol) to gave **3c** as orange needles (0.062 g, 39%) m.p.: 183–185 °C dec.; ¹H NMR (500 MHz [D₆]DMSO): δ = 3.30 (s, 3H, NCH₃), 3.95 (s, 3H, N⁺CH₃), 7.09 (m, 1H, ArH); 7.26 (d, J = 15.5 Hz, 1H, CH=CH); 7.26 (m, 1H, ArH), 7.45 (s, 1H, ArH), 7.54 (d, J = 8.5 Hz, 1H, ArH), 7.63 (d, J = 7.5 Hz, 1H, ArH), 7.86 (m, 1H, ArH), 8.12 (d, J = 15.5 Hz, 1H, CH=CH); 8.48 (t, J = 8.0 Hz, 1H, ArH), 8.70 (d,

$J = 7.5$ Hz, 1H, ArH), 8.87 ($t, J = 8.0$ Hz, 1H, ArH) ppm; ^{13}C NMR (126 MHz $[\text{D}_6]\text{DMSO}$): $\delta = 29.88, 47.79; 100.75, 109.13, 119.7, 120.44, 121.62, 122.02, 125.76, 127.38, 129.56, 131.21, 133.11, 136.34, 137.98, 145.87, 152.09$ ppm; MS (positive ESI): m/z (%): 249.3 $[\text{M} - \text{I}]^+$.

4.3.13. 4-[(E)-2-[4-(Dimethylamino)phenyl]vinyl]-1-methylpyridinium iodide [36], **4a**

The compound was synthesized according to the general procedure using 1,4-dimethylpyridinium iodide (0.470 g, 2 mmol) and 4-(dimethylamino)benzaldehyde (0.298 g, 2.00 mmol) to gave **4a** (0.513 g, 70%).

4.3.14. 1-Methyl-4-[(E)-2-(1-methyl-1H-pyrrol-2-yl)vinyl]pyridinium iodide [37], **4b**

The compound was synthesized according to the general procedure using 1,4-dimethylpyridinium iodide (0.470 g, 2 mmol) and 1-methyl-1H-pyrrole-2-carbaldehyde (0.218 g, 2.00 mmol) to gave **4b** (0.626 g, 96%).

4.3.15. 1,3-Dimethyl-2-[(E)-2-(1-methyl-1H-pyrrol-2-yl)vinyl]-1H-imidazol-3-ium iodide, **5**

The compound was synthesized according to the general procedure using 1,2,3-trimethyl-1H-imidazol-3-ium iodide (0.100 g, 0.043 mmol) and 1-methyl-1H-indole-2-carbaldehyde (0.065 g, 0.043 mmol) to gave **5** as yellow needles (0.071 g, 44%) m.p.: 310–312 °C; ^1H NMR (500 MHz $[\text{D}_6]\text{DMSO}$): $\delta = 3.57$ (s, 3H, NCH_3), 3.74 (s, 6H, N^+CH_3), 7.08 ($t, J = 8.0$ Hz, 1H, ArH), 7.22 ($t, J = 8.0$ Hz, 1H, ArH), 7.27 ($d, J = 16.5$ Hz, 1H, $\text{CH}=\text{CH}$); 7.30 (s, 1H, ArH), 7.53 ($d, J = 8.0$ Hz, 1H, ArH), 7.61 ($d, J = 8.0$ Hz, 1H, ArH), 7.65 ($d, J = 16.5$ Hz, 1H, $\text{CH}=\text{CH}$), 7.76 (s, 2H, ArH) ppm; ^{13}C NMR (126 MHz $[\text{D}_6]\text{DMSO}$): $\delta = 29.78, 36.73, 37.63, 58.08, 106.26, 111.49, 112.86, 119.15, 119.74, 121.61, 122.79, 130.47, 141.14, 156.65, 158.59, 166.68$ ppm; MS (positive ESI): m/z (%): 252.2 $[\text{M} - \text{I}]^+$.

4.4. Biological essays

4.4.1. Human cell lines (A549 and H226)

The human lung carcinoma cell line A549 (ATCC number: CCL-185) and the human lung squamous carcinoma cell line NCI-H226 (ATCC number: CRL-5826) were obtained from the American Type Culture Collection (ATCC, Teddington, UK). The cell lines were grown in RPMI 1640 medium supplemented with 10% (vol/vol) heat-inactivated foetal bovine serum, 2 mM L-Alanyl-L-Glutamine, penicillin-streptomycin (50 units–50 μg for ml) and incubated at 37 °C in humidified atmosphere of 5% CO_2 , 95% air. The culture medium was changed twice a week.

4.4.2. Treatment with antitumour compounds and MTT colorimetric assay

Human cancer cell line (5×10^3 cells/ 0.33 cm^2) were plated in 96 well plates “Nunc TM Microwell TM” (Nunc) and were incubated at 37 °C. After 24 h, cells were treated with the compounds (final concentration 0.01 – $100 \mu\text{M}$). Cells treated with 0.5–1% dimethyl sulfoxide (DMSO) were used as controls. Microplates were incubated at 37 °C in humidified atmosphere of 5% CO_2 , 95% air for 3 days and then cytotoxicity was measured with colorimetric assay based on the use of tetrazolium salt MTT (3-(4,5-dimethylthiazol-2-yl)-2,5-diphenyl tetrazolium bromide) [38]. The results were read on a multiwell scanning spectrophotometer (Multiscan reader), using a wavelength of 570 nm. Each value was the average of 8 wells (standard deviations were less than 10%). The GI_{50} value was calculated according to NCI: thus, GI_{50} is the concentration of test compound where $100 \times (T-T_0)/(C-T_0) = 50$ (T is the optical density of the test well after a 72 h period of exposure to

test compound; T_0 is the optical density at time zero; C is the DMSO control optical density). The cytotoxicity effect was calculated according to NCI when the optical density of treated cells was lower than the T_0 value using the following formula: $100 \times (T-T_0)/T_0 < 0$.

Acknowledgements

We thank the University of Catania for financial support.

Appendix. Supplementary information

Supplementary data related to this article can be found online at doi:10.1016/j.ejmech.2011.10.060.

References

- [1] F.P. Ballistreri, V. Barresi, P. Benedetti, G. Caltabiano, C.G. Fortuna, M.L. Longo, G. Musumarra, *Bioorg. Med. Chem.* 12 (2004) 1689–1695.
- [2] P.J. Goodford, *J. Med. Chem.* 28 (1985) 849–857;
- [3] G. Cruciani, K.A. Watson, *J. Med. Chem.* 37 (1994) 2589–2601.
- [4] R.D. Cramer III, D.E. Patterson, J. Bunce, *J. Am. Chem. Soc.* 110 (1988) 5959–5967.
- [5] M. Pastor, G. Cruciani, I. McLay, S. Pickett, S. Clementi, *J. Med. Chem.* 43 (2000) 3233–3243.
- [6] H. González-Díaz, G. Agüero, M.A. Cabrera, R. Molina, L. Santana, E. Uriarte, G. Delogu, N. Castañedo, *Bioorg. Med. Chem. Lett.* 15 (2005) 551–557.
- [7] H. González-Díaz, Y. Marrero, I. Hernandez, I. Bastida, E. Tenorio, O. Nasco, E. Uriarte, N. Castaneda, M.A. Cabrera, E. Aguila, O. Marrero, A. Morales, M. Perez, *Chem. Res. Toxicol.* 16 (2003) 1318–1327.
- [8] H. González-Díaz, M. Cruz-Monteagudo, R. Molina, E. Tenorio, E. Uriarte, *Bioorg. Med. Chem.* 13 (2005) 1119–1129.
- [9] E. Estrada, *Mutat. Res.* 420 (1998) 67–75.
- [10] H. González-Díaz, E. Olazábal, L. Santana, E. Uriarte, Y. González-Díaz, N. Castañedo, *Bioorg. Med. Chem.* 15 (2007) 962–968.
- [11] H. González-Díaz, L.A. Torres-Gómez, Y. Guevara, M.S. Almeida, R. Molina, N. Castañedo, L. Santana, E. Uriarte, *J. Mol. Model.* 11 (2005) 116–123.
- [12] H. González-Díaz, M. Cruz-Monteagudo, R. Molina, E. Tenorio, E. Uriarte, *Bioorg. Med. Chem.* 13 (2005) 1523–1530.
- [13] J.I. González Borroto, G. Pérez Machado, A. Creus, R. Marcos, *Mutagenesis* 20 (2005) 193–197.
- [14] C.G. Fortuna, V. Barresi, G. Berellini, G. Musumarra, *Bioorg. Med. Chem.* 16 (2008) 4150–4159.
- [15] C.G. Fortuna, V. Barresi, G. Musumarra, *Bioorg. Med. Chem.* 18 (2010) 4516–4523.
- [16] M. Tarleton, J. Gilbert, M.J. Robertson, A. McCluskey, J.A. Sakoff, *Med. Chem. Comm.* 2 (2011) 31–37.
- [17] C.G. Fortuna, C. Bonaccorso, F. Qamarb, A. Anu, I. Ledoux, G. Musumarra, *Org. Biomol. Chem.* 9 (2011) 1608–1613.
- [18] E. Carosati, S. Sciabola, G. Cruciani, *J. Med. Chem.* 47 (2004) 5114–5125.
- [19] P. Crivori, G. Cruciani, P.A. Carrupt, B. Testa, *J. Med. Chem.* 43 (2000) 2204–2216.
- [20] G. Cruciani, M. Meniconi, E. Carosati, I. Zamora, R. Mannhold, in: H. van de Waterbeemd, H. Lennernäs, P. Artursson (Eds.), *Methods and Principles in Medicinal Chemistry*, vol. 18, Wiley-VCH Publishers, 2003, pp. 406–419.
- [21] G. Berellini, G. Cruciani, R. Mannhold, *J. Med. Chem.* 48 (2005) 4389–4399.
- [22] R. Mannhold, H. Kubinyi, G. Folkers (Eds.), *Molecular Interaction Fields*, vol. 27, WILEY-VCH Verlag GmbH & Co. KGaA, Weinheim, 2006, pp. 173–196.
- [23] S. Wold, M. Sjöström, in: B.R. Kowalski (Ed.), *Chemometrics: Theory and Application*, ACS Symposium Series, Washington, 1977, pp. 243–282.
- [24] S. Wold, C. Albano, W.J. Dunn III, U. Edlund, K. Esbensen, P. Geladi, S. Hellberg, E. Johansson, W. Lindberg, M. Sjöström, in: B.R. Kowalski (Ed.), *Chemometrics* (1984), pp. 17–96.
- [25] www.moldiscovery.com.
- [26] GRID v. 20 Molecular Discovery Ltd.
- [27] D.N.A. Boobbyer, P.J. Goodford, P.M. McWhinnie, R.C. Wade, *J. Med. Chem.* 32 (1989) 1083–1094.
- [28] J.M. Kauffman, G. Moyna, *J. Org. Chem.* 68 (2003) 839–853.
- [29] X.H. Zhang, L.Y. Wang, Z.X. Nan, S.H. Tan, Z.X. Zhang, *Dyes Pigm.* 79 (2008) 205–209;
- [30] D. Sutherland, C. Compton, *J. Org. Chem.* 17 (1952) 1257–1261.
- [31] W.L. Foye, Y.J. Lee, K.A. Shan, J.M. Kauffman, *J. Pharm. Sci.* 67 (1978) 962–964.
- [32] C.F. Koelsch, *J. Am. Chem. Soc.* 66 (1944) 2126.
- [33] A.P. Phillips, *J. Org. Chem.* 14 (1949) 302–305.
- [34] D. Reefman, J.P. Cornelissen, J.G. Haasnoot, R.A.G. De Graaff, J. Reedijk, *Inorg. Chem.* 29 (1990) 3933–3935.
- [35] K. Chanawanno, S. Chantrapromma, T. Anantapong, A. Kanjana-Opas, H.-K. Fun, *Eur. J. Med. Chem.* 45 (2010) 4199–4208.
- [36] X. Xu, W. Qiu, Q. Zhou, J. Tang, F. Yang, Z. Sun, P. Audebert, *J. Phys. Chem. B.* 112 (2008) 4913–4917.

- [35] E. Marri, U. Mazzucato, C.G. Fortuna, G. Musumarra, A. Spalletti, J. Photochem. Photobiol. A 179 (2006) 314–319;
F.P. Ballistreri, V. Barresi, G. Consiglio, C.G. Fortuna, M.L. Longo, G. Musumarra, ARKIVOC 1 (2003) 105–117.
- [36] G.R. Clemo, G.A. Swan, J. Chem. Soc. (1938) 1454–1455.
- [37] A. Facchetti, A. Abbotto, L. Beverina, M.E. van der Boom, P. Dutta, G. Evmenenko, G.A. Pagani, T.J. Marks, Chem. Mater. 15 (2003) 1064–1072.
- [38] T.J. Mosmann, J. Immunol. Meth. 65 (1983) 55–63.